Quaternary Science Reviews 107 (2015) 231–242

Contents lists available at ScienceDirect

Quaternary Science Reviews

journal homepage: www.elsevier.com/locate/quascirev

Early break-up of the Norwegian Channel Ice Stream during the Last Glacial Maximum

John Inge Svendsen [a, *], Jason P. Briner [b], Jan Mangerud [a], Nicolás E. Young [c]

[a] Department of Earth Science, University of Bergen and Bjerknes Centre for Climate Research, Postbox 7803, N-5020 Bergen, Norway
[b] Department of Geology, University at Buffalo, Buffalo, NY 14260, USA
[c] Lamont-Doherty Earth Observatory, Columbia University, Palisades, NY, USA

ARTICLE INFO

Article history:
Received 11 June 2014
Received in revised form
31 October 2014
Accepted 3 November 2014
Available online

Keywords:
Norwegian Channel Ice Stream
Scandinavian Ice Sheet
^{10}Be dating
Last Glacial Maximum
Lateglacial
Western Norway

ABSTRACT

We present 18 new cosmogenic ^{10}Be exposure ages that constrain the breakup time of the Norwegian Channel Ice Stream (NCIS) and the initial retreat of the Scandinavian Ice Sheet from the Southwest coast of Norway following the Last Glacial Maximum (LGM). Seven samples from glacially transported erratics on the island Utsira, located in the path of the NCIS about 400 km up-flow from the LGM ice front position, yielded an average ^{10}Be age of 22.0 ± 2.0 ka. The distribution of the ages is skewed with the 4 youngest all within the range 20.2–20.8 ka. We place most confidence on this cluster of ages to constrain the timing of ice sheet retreat as we suspect the 3 oldest ages have some inheritance from a previous ice free period. Three additional ages from the adjacent island Karmøy provided an average age of 20.9 ± 0.7 ka, further supporting the new timing of retreat for the NCIS. The ^{10}Be ages from Utsira and Karmøy suggest that the ice stream broke up about 2000 years earlier than the age assignment based on ^{14}C ages on foraminifera and molluscs from marine sediment cores. We postulate that the Scandinavian Ice Sheet flowed across the Norwegian Channel to Denmark and onto the North Sea plateau during early phases of the LGM. When the NCIS started to operate this ice supply to the North Sea was cut off and the fast flow of the NCIS also led to a lowering of the ice surface along the Norwegian Channel and thereby drawdown of the entire ice sheet. This facilitated rapid calving of the ice front in the North Sea and we reconstruct a large open bay across the entire northern North Sea by ~20 ka based on our ^{10}Be ages in the east and radiocarbon ages from marine cores in the west. Additional ^{10}Be ages show that the mainland slightly east of the islands Utsira and Karmøy remained ice covered until about 16 ka, indicating almost no net ice-margin retreat for the 4000 years between 20 and 16 ka. After 16 ka the ice margin retreated quickly up-fjord.

1. Introduction

Ice streams are important components of ice sheets, influencing both their geometry and dynamic behaviour (Stokes and Clark, 2001; Bennett, 2003; Pritchard et al., 2009). Considering that they have the capacity to discharge large volumes of ice during short periods of time, they may potentially destabilize entire ice sheets and thus enforce fast eustatic sea-level rise (Alley et al., 2005; Pritchard et al., 2009). In this respect the Norwegian Channel Ice Stream (NCIS) may offer some insights into both ice-sheet dynamics and forcing mechanisms (Ottesen et al., 2005; Sejrup et al., 2003, 2009). Here, we also point out implications that may have bearing on the causal connection for such early deglaciation of the NCIS.

The Norwegian Channel is an 800-km-long and 50- to 100-km-wide glacially eroded trough that trends along the coast of southern Norway terminating at the shelf break in the northern North Sea (Figs. 1 and 2). During Quaternary glaciations, this trough hosted a major ice stream that drained a large part of the Scandinavian Ice Sheet over southern Norway and Sweden (Sejrup et al., 2003, 2009). The time frame for the last break-up of the NCIS so far has been established by radiocarbon dating of foraminifera and molluscs from marine sediment cores. These ages suggest that the ice front started to retreat from the shelf break at ~19 ka (King et al., 1998; Sejrup et al., 2009) and reached inside the Troll oil field area not later than ~18.5 ka (Fig. 2; Sejrup et al., 2009). In this paper

* Corresponding author. Tel.: +47 55583510.
E-mail address: John.Svendsen@geo.uib.no (J.I. Svendsen).

http://dx.doi.org/10.1016/j.quascirev.2014.11.001
0277-3791/

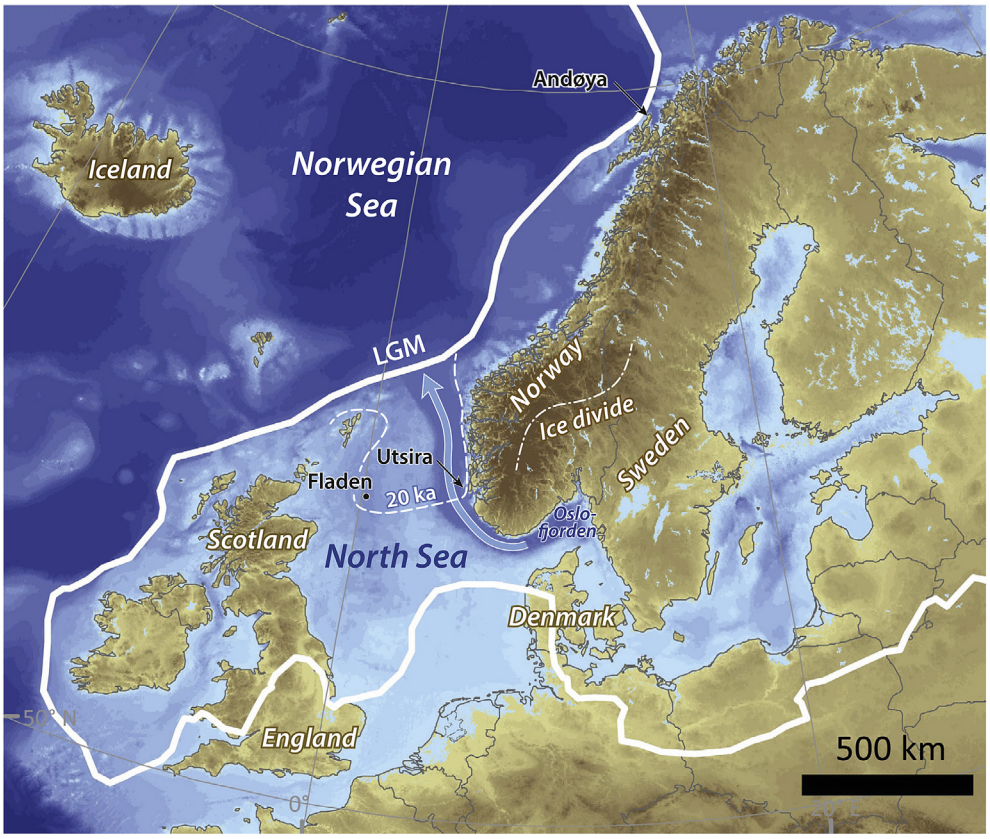

Fig. 1. Overview map of NW Europe. The map shows the Last Glacial Maximum (LGM) extent of the Scandinavian and British Ice Sheets; ice margin not time synchronous [modified from Svendsen et al. (2004) and Clark et al. (2012)]. The Norwegian Channel Ice Stream is marked with an arrow. Dashed white lines show schematically a possible reconstruction of the ice margin about ~20 ka accepting that both Utsira and the Fladen Ground area were ice free at this time.

we present a series of cosmogenic ^{10}Be exposure ages (hereafter ^{10}Be ages) from glacially transported boulders on the islands Utsira and Karmøy that are situated near the eastern flank of the Norwegian Channel in south-western Norway (Table 1; Figs. 2 and 3). The ^{10}Be ages from these islands reveal that the ice front had retreated 400 km up-stream from its LGM position by ~20 ka, about 2000 years earlier than suggested by the data from marine sediment cores. We also present several ^{10}Be ages from sites on the adjacent mainland suggesting that these coastal areas remained ice covered until ~16 ka, at which time the wide embayment of Boknafjorden became permanently ice free. In a companion study we have dated the further ice sheet retreat towards the inner fjord and mountain areas (Briner et al., 2014).

2. Glacial geologic setting and sample locations

The Norwegian Channel starts at the mouth of Oslofjorden and extends along the west coast of Norway throughout our study area between Jæren and the shelf break (Figs. 1 and 2). The shelf-crossing channel is eroded into relatively soft Mesozoic sedimentary strata that verge onto crystalline rocks near the landward margin (Rise et al., 2008). The frequent occurrence of glacial striae on land show that ice flow was directed almost due west during the maximum ice sheet extent (e.g., Aarseth and Mangerud, 1974; Holtedahl, 1975), but lineations that are recorded on the adjacent sea floor show that the ice flow turned northward and merged with the NCIS a short distance beyond the coastline (Sejrup et al., 1998).

The deglaciation of the northern segment of the Norwegian Channel between the shelf margin and the Troll site (Fig. 2) is previously considered to have taken place between 19 and 18.5 ka (Sejrup et al., 2009). After this retreat of the NCIS, the western margin of the Scandinavian Ice Sheet remained along the outer coast for several thousand years before it continued to retreat towards the east (Mangerud et al., 2013). We used ^{10}Be dating on 18 rock samples from coastal areas in the county of Rogaland, south-western Norway (Figs. 2 and 3; Table 1). This includes 12 samples that were collected on the islands Utsira and Karmøy and six samples from sites located in Tananger and Våg on the mainland in the Boknafjorden area (Fig. 3). A description of each sampling area is provided below.

2.1. Utsira

Utsira is a small island, only 3 km across, located in the open ocean to the west of the town of Haugesund (Figs. 1–3). It is situated on the inner shelf just east of the Norwegian Channel, about 400 km to the south of the shelf break and the LGM limit of the Scandinavian Ice Sheet (Fig. 3). All glacial striae that have previously been reported from the island reflect an ice flow that was directed towards the north (Undås, 1948). During fieldwork we searched for glacial striae in various parts of the island, especially on the east coast, to determine if there was younger ice flow from the east, i.e. a glacial imprint from the period after the ice stream collapsed. However, like previous investigators, we found only diffuse striations directed towards the north (350-010°). We therefore assume that Utsira was overridden by the NCIS just prior to the last deglaciation.

Utsira is unique in the sense that it is the only island along the coast that is located within the track of the last NCIS and it was not affected by ice flow from the east during deglaciation. We thus

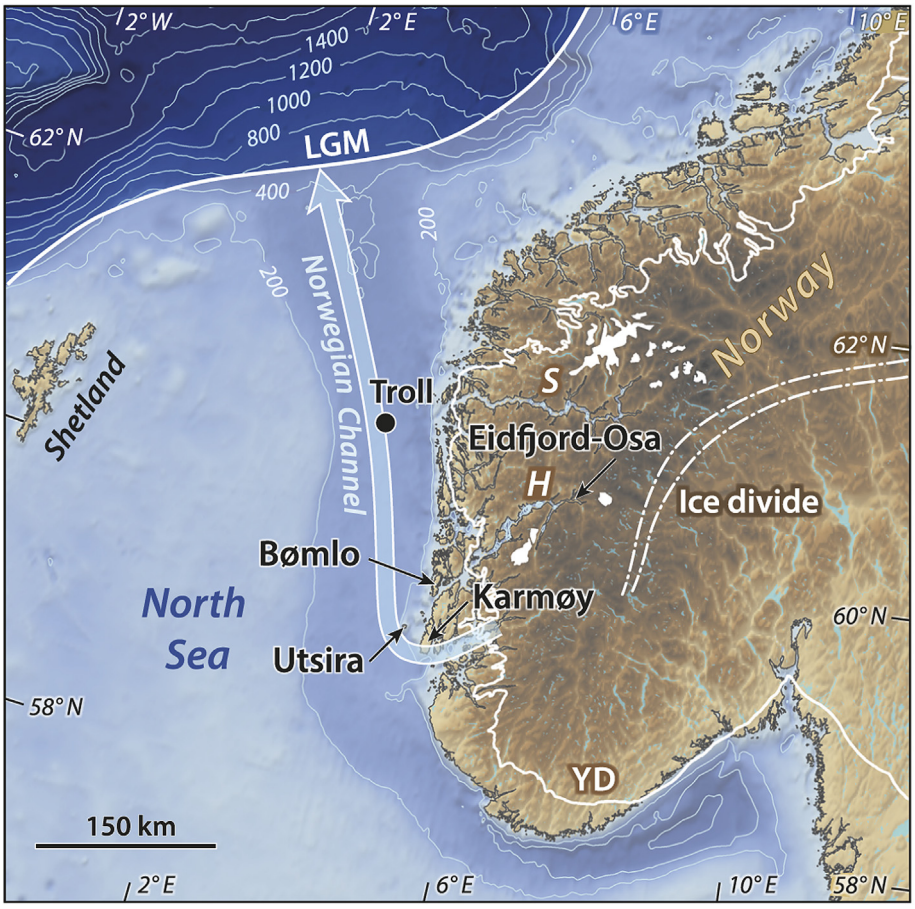

Fig. 2. Map of Southern Norway and the adjacent North Sea. The maps show the extent (marked LGM) and approximate position of the ice divide of the Scandinavian Ice Sheet during the Last Glacial Maximum (LGM). The Younger Dryas ice limit is marked with a white line on land. White fields are present day glaciers. The white arrow shows the flow path for ice out of Boknafjorden and into the Norwegian Channel during LGM and also represents the profile line used in Fig. 8.

consider that the erratics on the island were left behind by the retreating NCIS therefore making them suitable to date the deglaciation of the Norwegian Channel. The island is characterized by a rocky terrain spanning up to the highest hill at an elevation of 65 m a.s.l. The Quaternary sediment cover is patchy and consists mostly of peat and some infill of shallow marine sediments in the low-lying depressions. Undås (1948) considered the marine limit to be about 30 m a.s.l., but the highest shorelines that we could recognize in the field are beach ridges at 10–12 m a.s.l. that most likely formed during the culmination of the mid-Holocene sea-level rise (Tapes transgression) that affected the outermost coast (Hafsten, 1983). We assume that highest sea-level stand on Utsira during the Lateglacial period did not exceed this level. Some areas on Utsira are strewn with large glacial erratics, for the most part derived from the local bedrock made up of Caledonian igneous rocks that in this area is are dominated by diorites and gabbros (Ragnhildstveit et al., 1998). We dated seven samples from large glacially transported boulders and one from an ice-moulded bedrock surface (Table 1, Figs. 3 and 4).

2.2. Karmøy

Karmøy is a 30-km-long island that is located 14 km to the southeast of Utsira (Fig. 3). Most of the interior of the island is located between 50 and 100 m a.s.l. and this central "plateau" is flanked by a lower rim of land that most places is bounded by an inner escarpment at about 30–40 m a.s.l. The marine limit is probably 13–14 m a.s.l. in the south rising to about 23 m in the northernmost part of the island (Austad and Eriksen, 1987). All reported glacial striations are directed almost due west and a similar ice movement has also been inferred from till fabric analysis (Ringen, 1964). This pattern is also consistent with our own field observations on Karmøy. Thus, the pattern of glacial striae indicates that the eastern boundary of the NCIS was located between Utsira and Karmøy and there seems to have been a sharp bend in the ice flow direction in the area between the two islands. We collected samples from Karmøy to determine the age relation between the breakup of the NCIS and ice retreat across the outer coast. We collected four samples near the farm Haga on the southwestern side of Karmøy (Fig. 3); three samples were collected from boulders and one from an ice-moulded bedrock surface that in this area consists of granite and granodiorite (Ragnhildstveit et al., 1998).

2.3. Tananger

The Tananger sample site is located near the northern tip of Jæren, nearly 30 km to the southeast of Karmøy, across the mouth of Boknafjorden (Fig. 3). The last ice flow here was directed towards the W–SW. Three samples (two glacially transported boulders and one sample from striated bedrock) were dated from the summit of a low rocky hill called Søre Varåsen at 60–65 m a.s.l., a few km to the southwest of Stavanger. The marine limit in this area is about 17 m

Table 1
^{10}Be sample data and ages.

Sample	Sample type	Sample height (m)	Boulder dimension (m)	Lat. (°N)	Long. (°E)	Elevation (m a.s.l.)	Sample thick. (cm)	Top. shield. factor	^{10}Be concentration	^{10}Be age (ka)[a]	^{10}Be age corrected for uplift[b]	^{10}Be age using Arctic-wide PR[c]
Utsira												
41-11NOR-5	boulder	3.0	4.0 × 6.0	59° 18.823′	4° 53.619′	34	3	1	109,029 ± 2618	25.0 ± 0.6	25.1 ± 0.6	25.8 ± 0.6
41-11NOR-3	boulder	1.3	3.0 × 3.0	59° 18.578′	4° 54.096′	23	2	1	105,033 ± 3218	24.2 ± 0.7	24.3 ± 0.7	25.0 ± 0.8
41-11NOR-1	boulder	0.6	1.3 × 1.5	59° 18.249′	4° 52.425′	50	1	1	101,825 ± 2270	22.6 ± 0.5	22.6 ± 0.5	23.3 ± 0.5
46-11NOR-2	boulder	2.5	2.0 × 2.0	59° 18.022′	4° 52.222′	42	3.5	1	091,329 ± 3692	20.8 ± 0.8	20.9 ± 0.8	21.5 ± 0.9
44-11NOR-4	boulder	2.5	3.0 × 4.0	59° 18.722′	4° 53.803′	38	0.5	1	090,477 ± 1792	20.2 ± 0.4	20.3 ± 0.4	20.9 ± 0.4
41-11NOR-9	boulder	1.0	3.0 × 2.0	59° 18.649′	4° 53.987′	28	2	1	088,339 ± 2598	20.2 ± 0.6	20.3 ± 0.6	20.9 ± 0.6
41-11NOR-7	boulder	1.0	1.5 × 1.5	59° 18.764′	4° 54.001′	29	1.5	1	088,590 ± 2911	20.2 ± 0.7	20.2 ± 0.7	20.8 ± 0.7
41-11NOR-6	bedrock	0	–	59° 18.802′	4° 53.998′	52	2	1	181,978 ± 3780	40.8 ± 0.9	41.1 ± 0.9	42.1 ± 0.9
Karmoy												
45-11NOR-53	boulder	1.2	2.0 × 0.5	59° 11.093′	5° 11.711′	81	3	1	101,877 ± 3083	22.2 ± 0.7	22.3 ± 0.7	23.0 ± 0.7
45-11NOR-54	boulder	1.25	2.0 × 2.0	59° 11.062′	5° 11.694′	81	3	1	093,088 ± 2536	20.3 ± 0.6	20.4 ± 0.6	21.0 ± 0.6
45-11NOR-56	boulder	1.5	4.0 × 4.0	59° 11.033′	5° 11.961′	91	2.5	1	093,242 ± 1913	20.0 ± 0.4	20.1 ± 0.4	20.7 ± 0.4
44-11NOR-55	bedrock	0	–	59° 11.058′	5° 11.700′	77	1	1	442,731 ± 8227	97.2 ± 1.9	97.8 ± 1.9	100.6 ± 1.9
Tananger												
41-11NOR-36	bedrock	0	–	58° 54.930′	5° 36.628′	64	1	1	074,241 ± 1399	16.2 ± 0.3	16.4 ± 0.3	16.8 ± 0.3
41-11NOR-35	boulder	3.0	5.0 × 4.0	58° 54.913′	5° 36.636′	65	2.5	1	071,735 ± 1875	15.8 ± 0.4	16.1 ± 0.4	16.4 ± 0.4
41-11NOR-34	boulder	2.0	4.0 × 2.0	58° 54.998′	5° 36.938′	60	1.2	1	070,941 ± 1401	15.6 ± 0.3	15.8 ± 0.3	16.1 ± 0.3
Våg												
45-11NOR-59	bedrock	0	–	59° 27.651′	5° 28.623′	89	4	0.999	075,416 ± 2278	16.4 ± 0.5	16.6 ± 0.5	17.0 ± 0.5
44-11NOR-60	boulder	1.0	2.5 × 2.0	59° 27.654′	5° 28.591′	87	1.5	0.999	075,138 ± 1836	16.1 ± 0.4	16.3 ± 0.4	16.6 ± 0.4
44-11NOR-61	boulder	1.3	2.0 × 2.0	59° 27.697′	5° 28.549′	87	6	0.999	070,658 ± 2073	15.7 ± 0.5	15.9 ± 0.5	16.2 ± 0.5

Notes: All samples with a rock density of 2.65 g cm^{-3}; zero rock surface erosion.
[a] Western Norway production rate (Goehring et al., 2012; calculated using CRONUS Earth website): http://hess.ess.washington.edu/math/al_be_v22/alt_cal/alt_cal.html.
[b] Same as for (a) but with corrections for isostatic rebound, using time-averaged elevation.
[c] Arctic-wide production rate value is 3.96 ± 0.15 (Young et al., 2013; no uplift; calculated using CRONUS Earth website): http://hess.ess.washington.edu/math/al_be_v22/alt_cal/alt_cal.html.

a.s.l. (Thomsen, 1981). We collected samples from this area to date the initial ice sheet retreat in Boknafjorden and the adjacent land mass.

2.4. Våg

The Våg site is situated on the mainland north of Boknafjorden about 35 km to the northeast of our sampling area on southern Karmøy (Fig. 3). The samples were collected from a low hill next to the main road (E39) near the head of Grindafjorden–Skjoldfjorden, a narrow and windy tributary to Boknafjorden. The sampling area is located around 14 km beyond the Younger Dryas ice sheet margin in Yrkjefjorden (Anundsen, 1985). The marine limit in Våg is about 35 m a.s.l. (Anundsen, 1985). The bedrock surface at the field site is sculpted by glacial erosion reflecting a westerly ice flow direction. Two samples were collected from glacially transported boulders and one from a striated bedrock surface. Considering the location, we assume that a substantial portion of Boknafjorden was ice-free at the time when the Våg area was deglaciated.

3. Methods

We dated four samples from bedrock surfaces and 14 samples from perched boulders sitting on exposed bedrock mounds (Fig. 4, Table 1). We sampled the topmost few centimetres of the rock surfaces using a hammer and chisel. Almost all samples were collected from nearly horizontal surfaces and we avoided edges and places where the primary surfaces appear to have been weathered or eroded. We used clinometers to measure topographic shielding and a hand held GPS receiver to determine sample location and elevation. The altitude of the various sample locations range from ~23 to ~91 m a.s.l. and we are confident that all samples were collected from above the local marine limit. The collected rock material was prepared for ^{10}Be analysis at the University at Buffalo Cosmogenic Nuclide Laboratory. Following crushing, sieving and quartz isolation, samples were digested and beryllium isolated following procedures described in Young et al. (2013). Samples were prepared in batches of 12 that each included one process blank; all samples were spiked with ~0.65–0.70 g of 405 ppm ^{9}Be carrier. ^{10}Be/^{9}Be ratios were measured at the Center for Mass Spectrometry, Lawrence Livermore National Laboratory and normalized to standard 07KNSTD3110 with a reported ratio of 2.85×10^{-12} (Nishiizumi et al., 2007; Rood et al., 2010). Procedural blank ratios were 9.56×10^{-16}, 9.63×10^{-16}, 1.22×10^{-15} and 1.79×10^{-15}, equating to background corrections of 0.26–1.58% of the sample total. One-sigma analytical uncertainties on background-corrected samples range from 1.9 to 4.0% and average 3.3 ± 0.6% (Table 1).

The ^{10}Be ages were calculated using the CRONUS-Earth online exposure age calculator (Balco et al., 2008; version 2.2 constants 2.2). We adopted a regionally constrained production rate from southwestern Norway (Goehring et al., 2012) with the Lal/Stone constant-production scaling scheme to calculate ^{10}Be ages (Lal, 1991; Stone, 2000). We use this scaling scheme because the influence of the Earth's magnetic field on ^{10}Be production rate is considered to be negligible at the study area's high latitude (°59 N; Gosse and Phillips, 2001); use of alternative scaling schemes results in ^{10}Be ages that vary by up to ~6%. The CRONUS-Earth calculator makes sample-specific corrections for latitude, elevation, sample thickness and sample density (2.65 g cm^{-3}; Table 1). Reported age uncertainties for individual samples reflect 1-sigma AMS uncertainty only ("internal" uncertainty reported from the CRONUS-Earth website; http://hess.ess.washington.edu/). We made no corrections for surface erosion. The crystalline bedrock in the region is fairly resistant to erosion, and glacial striations were routinely observed on many of the sample surfaces. The field area has undergone isostatic adjustment since deglaciation, and the sample elevation at the time of collection does not reflect its time-averaged sample elevation history. However, influence of isostatic uplift on the ^{10}Be ages may be offset by unquantifiable effects of atmospheric

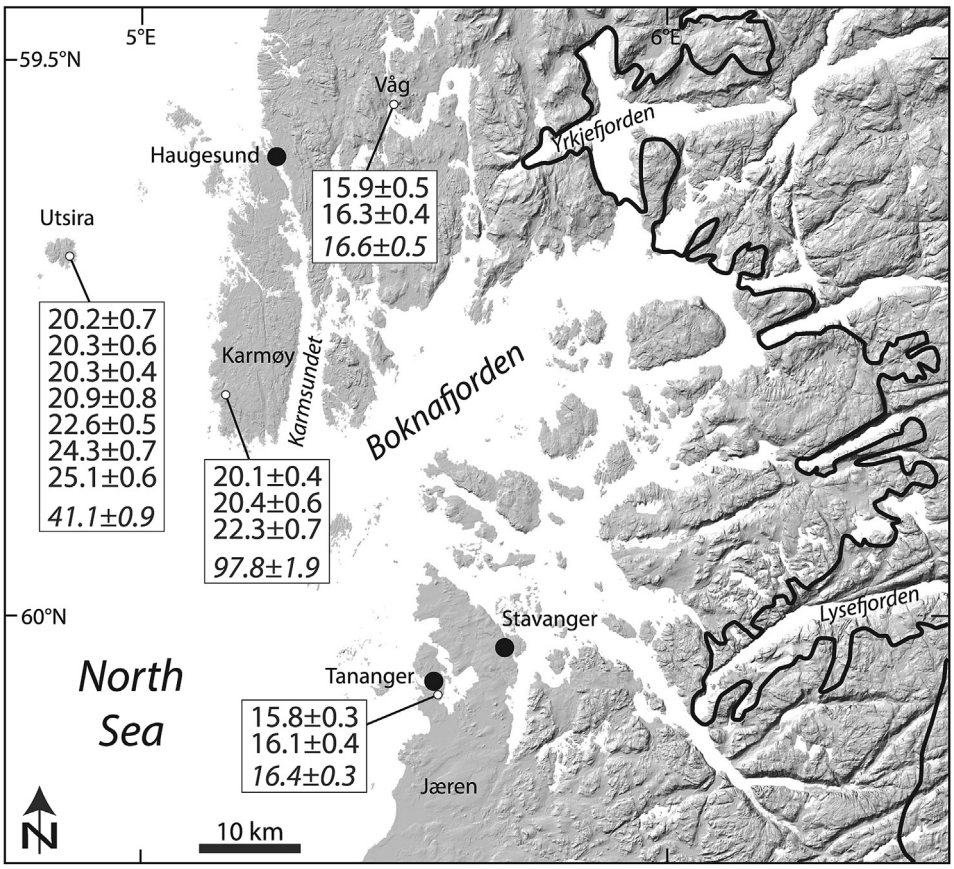

Fig. 3. Map of the study area in the Boknafjorden region. The map shows the location of ^{10}Be ages (ka) and the extent of the Scandinavian Ice Sheet during the Younger Dryas (black line; Andersen et al., 1995; Anundsen, 1989). ^{10}Be ages in plain text are from boulders, ages in italic text are from bedrock surfaces.

pressure changes related to ice sheet proximity and glacial-world atmospheric compression (Staiger et al., 2007). The ages we report below are adjusted for uplift, but we report both "raw" and "uplift-corrected" ages in Table 1. For the uplift-corrected ages, we use relative sea-level data from Anundsen (1985, 1989), Thomsen (1981) and Helle (2006). We note that ^{10}Be ages corrected for isostatic uplift are ~0.3–1.3% older than the uncorrected ages, and thus the correction does not significantly influence our chronology.

4. Results

All dated boulders from the islands Utsira and Karmøy yielded ^{10}Be ages between 25.1 ± 0.6 and 20.1 ± 0.4 ka, whereas the boulders from the mainland sites Tananger and Våg gave significantly younger ages between 16.1 ± 0.4 and 15.8 ± 0.3 ka (Figs. 3, 5 and 6; Table 1). The two samples that were collected from exposed bedrock surfaces on Utsira and Karmøy gave much older ages of 41.1 ± 0.9 and 97.8 ± 1.9 ka, respectively, than those from the erratics (Table 1). The two old ^{10}Be ages from Utsira and Karmøy are of interest when considering the local glacial erosion rates and potential for inheritance of ^{10}Be in boulders, but they are much too old to represent deglaciation.

The seven ^{10}Be ages from boulders on Utsira have a skewed distribution with the three youngest samples having identical ages that average 20.3 ± 0.1 ka; the four youngest ages average 20.4 ± 0.3 ka (Figs. 5 and 6). This distribution of ages is typical for populations where some samples have inheritance stemming from foregoing ice-free periods (Applegate et al., 2012), suggesting that the clustering of youngest ages more faithfully represents the true age of deglaciation than the average age (22.0 ± 2.0 ka) of all erratics. That the sample population is influenced by some inheritance from a previous ice-free period is somewhat expected given the inherited ^{10}Be inventory in the local bedrock (apparent ^{10}Be age of 41.1 ± 0.9 ka) and the fact that the erratics on Utsira are mostly locally derived. Judged from the whole series of ^{10}Be ages we conclude that Utsira became deglaciated at ~20 ka. We note that this is the youngest possible age that can be taken from our data set and yet the one in least conflict with the existing radiocarbon-based ages for deglaciation. If all ages are given equal weight, it would shift the timing of deglaciation farther back in time and increase the mismatch with the marine radiocarbon ages.

The three boulders that we dated from Karmøy gave almost similar ages (20.1 ± 0.4, 20.4 ± 0.6 and 22.3 ± 0.7 ka) with a mean value of 20.9 ± 1.2 ka (Table 1, Figs. 3, 5 and 6), but one sample gave a slightly older age (22.2 ± 0.7 ka) as compared to the two others that have identical ages (20.3 ± 0.6 and 20.0 ± 0.4 ka). The samples from Karmøy are similar to those from Utsira in many ways: the bedrock contains inheritance, the erratic boulders are perched directly on bedrock and there is no evidence of any post-deposition modification. Thus, considering the possibility that the oldest age may reflect some inheritance from a previous ice free period we place more confidence on the two youngest samples and conclude that the sampling area on Karmøy became ice free soon after Utsira.

The mean ages from the sites Tananger and Våg on the mainland are 16.1 ± 0.3 (n = 3) and 16.3 ± 0.4 ka (n = 3), respectively (Figs. 5 and 6). All ages from these and other areas along the coast farther to the north (Mangerud et al., 2013) are significantly younger than the samples from Utsira and Karmøy. The multiple ^{10}Be ages from each

Fig. 4. Sampling for ^{10}Be dating. The photographs show examples of boulders from the four field sites used for ^{10}Be dating. The samples are numbered as in Table 1.

of the Tananger and Våg sites overlap within one standard deviation and there is no tail of older ages. Unlike on Utsira or Karmøy, there is no evidence that bedrock at Tananger and Våg has inheritance, as the bedrock ages are identical to the boulder ages. Thus, we average all ^{10}Be ages from the Tananger and Våg sites to represent the deglaciation at these locations.

5. Discussion

The main goal of this work is to determine when the NCIS retreated from the outer Norwegian Channel and to date the deglaciation of the adjacent mainland. Our ^{10}Be ages suggest that the NCIS margin had retreated to Utsira at ~20 ka, which is about two thousand years earlier than previously thought from available radiocarbon ages from offshore sediment cores. We will therefore first assess the reliability of our ^{10}Be chronology and then discuss some of the implications of the early deglaciation history.

5.1. Reliability of the ^{10}Be chronology

All boulders that are dated as part of this study were large, glacially transported erratics resting directly on exposed bedrock surfaces (Fig. 4). Considering their geographic positions and geomorphological setting we can more or less rule out the possibility that they have turned around or moved after they were left on the ground by the retreating ice sheet. In general the topographic shielding of the cosmic radiation is minimal (Table 1), and the smooth character of the surfaces suggests minimal surface erosion has occurred since deposition. The boulders are located on top of bedrock mounds and possible shielding effects due to snow cover or vegetation are most certainly negligible. The shielding effect may potentially contribute to underestimate the true exposure ages, but it should be noted that the production rate that we use is determined from similar boulders and settings in western Norway. In conclusion, we are confident that processes causing too young ages are insignificant, except that our ^{10}Be ages could be influenced by fluctuating air pressure operating in ice-sheet marginal environments. Lower atmospheric pressure near ice-sheet margins due to katabatic wind effects and/or atmospheric compression would result in higher site-specific production rates (e.g. Stone, 2000; Staiger et al., 2007). Our sampling sites at Utsira and Karmøy were likely resting near the ice terminus for ~4000 years (see chronology below) and thus may have experienced higher production rates during this period. This effect would make our ^{10}Be ages from Utsira and Karmoy slightly younger and thus more in agreement with existing radiocarbon ages. However, because this potential effect is difficult to quantify and cannot completely explain the discrepancy between our ^{10}Be age and existing radiocarbon ages, we prefer to present and discuss our ^{10}Be ages without considering changing air pressure. We realize that this is a potential source of error that should be tested in future research, but as discussed below there is a close correspondence between ^{10}Be and ^{14}C ages from Norway.

As an independent test of the accuracy of the ^{10}Be ages, we compare ^{10}Be and radiocarbon ages from sites throughout western Norway (Fig. 7). First, on the island Andøya in northern Norway

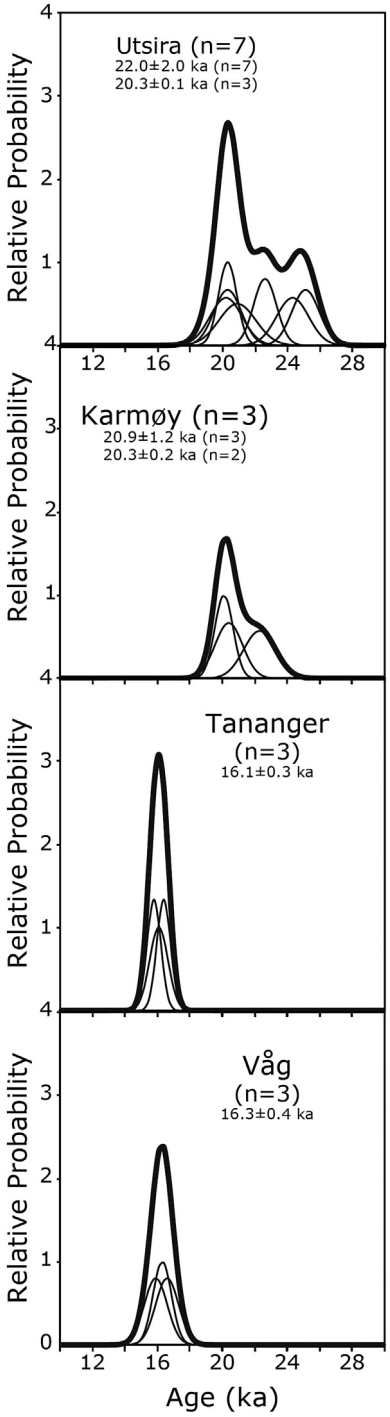

Fig. 5. Probability distribution of ^{10}Be ages of erratics. The graphs are normal kernel density estimates of ^{10}Be age populations from the field sites; thin lines are individual sample ages, black lines are summed probability. Values reported are mean age and one standard deviation uncertainty. The vertical axis shows a relative probability. As appear from the discussion in text, we suspect that the oldest ages from Utsira slightly overestimate the real age of the deglaciation as we suspect they have some inheritance from an older ice free period.

(Fig. 1), a radiocarbon dated lacustrine sequence indicated that the final deglaciation took place shortly before 22 ka (Vorren et al., 2013). Two samples from erratics on the adjacent Kjølhaug and Endletvatn moraine ridges yielded ^{10}Be ages of 24.2 ± 2.1 and 22.5 ± 2.2 ka when recalculated in the same way as the samples that we have analyzed as part of this study. Second, our ^{10}Be ages from Tananger are comparable with a series of radiocarbon ages of 17–16 ka from the basal lacustrine sediments from the Jæren region (Knudsen, 2006). Third, ^{10}Be ages from southern Bømlo (Mangerud et al., 2013) correspond with radiocarbon ages from basal lacustrine sediments from the same island (Karlsen, 2009). Fourth, the Younger Dryas moraine in Hardangerfjorden is precisely dated by ^{14}C ages of distal sediments (Lohne et al., 2011) and by ^{10}Be ages from boulders on an associated lateral moraine (Mangerud et al., 2013). Note that we have omitted the boulders on the end moraine that were used to determine the production rate that we apply (Goehring et al., 2012). Fifth, ^{10}Be ages from the Eidfjord–Osa Moraine are compared with radiocarbon ages of the same event (Mangerud et al., 2013). Overall there is a very close correspondence between ^{10}Be and radiocarbon ages, substantiating the accuracy of the ^{10}Be ages (Fig. 7). It should be noted that most alternative ^{10}Be production rate values (e.g. Balco et al., 2009), including the Arctic-wide value (Young et al., 2013), would make the ^{10}Be ages ~4% older (Table 1). For example, applying the Arctic-wide production rate would shift the exposure ages from Utsira and Karmøy to about 800 years older; thus, our ^{10}Be dating results are consistent with available stratigraphic data, but we still plan to test these results with further lake coring and radiocarbon dating.

5.2. Early collapse of the Norwegian Channel Ice Stream

The Scandinavian Ice Sheet was growing during the final stage of MIS 3 and may have reached a first glacial maximum as early as 29–27 ka (Houmark-Nielsen and Kjær, 2003; Larsen et al., 2009) at which time the ice from Norway coalesced with the British Ice Sheet in the North Sea (Clark et al., 2012). The configuration and chronology of the ice margins in the North Sea are still poorly known (Clark et al., 2012), but the Scandinavian Ice Sheet seems to have reached both Denmark (Larsen et al., 2009) and the mouth of the Norwegian Channel by about 23 ka (Nygard et al., 2007; Sejrup et al., 2009). Based on radiocarbon ages from offshore cores and seismic profiles it has been concluded that the NCIS started to withdraw from the mouth of the Norwegian Channel at around 20–19 ka (King et al., 1998; Nygard et al., 2007) and that the ice front reached the Troll site shortly before 18.5 ka (Sejrup et al., 2009). As opposed to the marine data from offshore sediment records, our ^{10}Be chronology indicates that the ice margin had retreated all the way to Utsira, a distance of 400 km from the mouth of the Norwegian Channel and 175 km south of the Troll site, as early as ~20 ka (Figs. 2 and 8). If correct, the radiocarbon ages from marine sediment cores at the Troll site slightly underestimate the real age for the collapse of the ice stream. We cannot offer a satisfying explanation for the deviating chronologies, but it should be noted that the basal dates from the Troll cores, which were conducted on foraminifers from the marine sediments covering the till, in principle provide only minimum ages of the ice sheet retreat. For example, one cannot exclude the possibilities that younger foraminifers have been mixed into the basal sediments and/or that there is a hiatus between the dated level and the till. If both deglaciation chronologies are correct the explanation must be that the Troll site was covered by a younger ice sheet advance from land (from the east), but without reaching Utsira farther to the south. However, we are not aware of geological observations in support of this possibility and in view of the available observations from the sea floor we are sceptical about this alternative explanation. When discussing the chronology one should also be aware of the possibility that the mismatch between the existing ^{14}C- and ^{10}Be chronologies may be less than 2000 years when taking into account the statistical measuring uncertainties and other potential errors connected with the two very different dating methods.

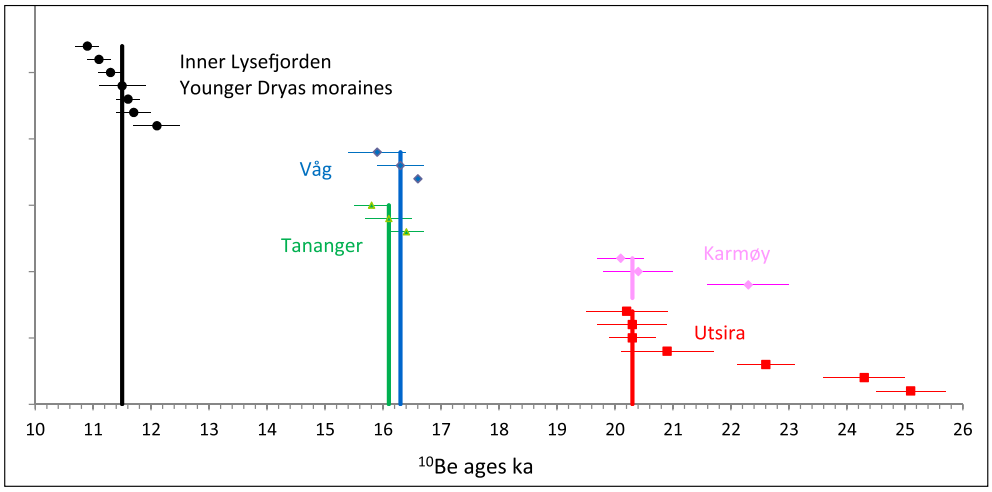

Fig. 6. ^{10}Be ages from the field sites. The ages are plotted with $\pm 1\sigma$ error bars; here also compared with ^{10}Be ages of the Younger Dryas moraine in Lysefjorden (Briner et al., 2014). Vertical bars show the concluded age for each site; for simplicity without errors. Note the distinct age difference between Utsira–Karmøy on the one side and Tanager–Våg on the other. The *y*-axis is only used to separate the samples so they are easier to see and has no further meaning.

The oldest radiocarbon ages from Utsira and Karmøy range from 16 to 17 ka and stem from sediment cores that were retrieved from lake basins above the marine limits (Paus, 1989a; 1990). These ages are significantly younger than our ^{10}Be ages; however, the radiocarbon-dated horizons are underlain by thick sequences of minerogenic silt and clay. Judged from the pollen stratigraphy, these lower sediment units correspond with a long-lasting, but undated cold period that came to an end at the onset of the Bølling interstadial when more organic sediments started to accumulate in response to a warmer climate (Paus, 1988; 1989a, 1990). Thus, even though our chronology remains to be confirmed by radiocarbon dating, the ^{10}Be dating results are consistent with the available stratigraphic data.

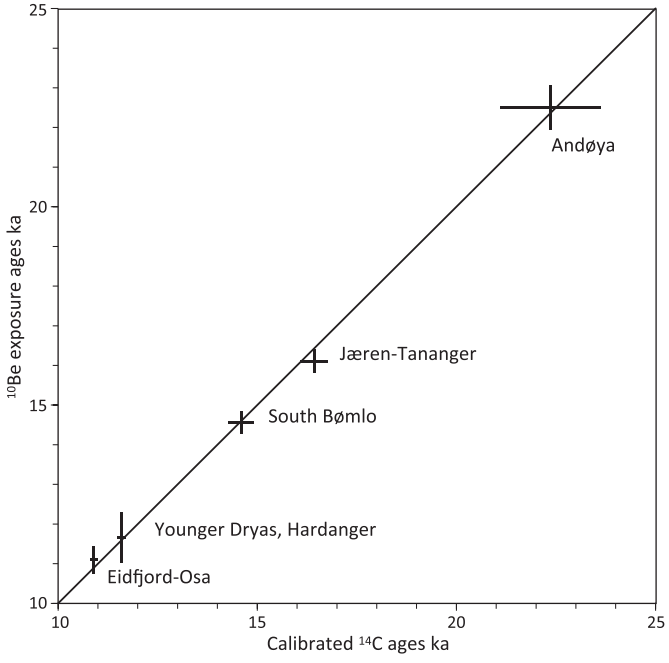

Fig. 7. ^{10}Be ages versus ^{10}C ages. The obtained ages of erratic boulders are plotted versus calibrated ^{14}C ages from terrestrial organic matter from lacustrine sediments that are assumed to have the same age as the boulders. All sites are located in western Norway, see description in text. The close correspondence between the two sets of ages supports the accuracy of ^{10}Be ages.

A rapid southward ice recession along the Norwegian Channel due to calving is considered a plausible pattern for the retreat. Considering that Utsira and Karmøy are located nearly 400 km to the south of the LGM ice margin imply that the ice stream must have broken up very fast shortly before 20 ka. This may have led to a narrow embayment that was constricted by the margins of the Norwegian Channel proper. However, it is noteworthy that several radiocarbon ages from cores from the Witch Ground Basin in the Fladen area, about 300 km to the west of Utsira (Fig. 1), suggest that this area became ice free as early as 27–25 cal ka (Sejrup et al., 1994, 2009, in press; Graham et al., 2010). Mainly relying on the ages from one of these cores (77/2), it has been proposed that a narrow marine embayment opened from the north between the British and Scandinavian ice sheets at ~25 ka and remained as a narrow bay until ~19 ka (Clark et al., 2012; Sejrup et al., 1994, 2009). In the light of the new ^{10}Be ages from Utsira and Karmøy, we find it glaciologically more likely that the entire stretch between Fladen and Utsira was ice free at ~20 ka. Since we do not have any new observations from the North Sea floor, we will not discuss the glacial history in detail, but point out two alternative reconstructions: The first is that Utsira and Fladen were located in a wide marine bay in the northern North Sea at ~20 ka (Fig. 1), and the second is that there was an ice-free "corridor" from north to south across the entire North Sea as early as ~20 ka. We note that the geometry of our reconstructed bay is rather similar to the one shown in Fig. 11 in Bradwell et al. (2008) that was based on moraines and other glacial elements, except that we extend it to the coast of Norway and that they did not assign a definite age to the embayment. Clark et al. (2012) reconstructed an embayment very similar to ours in their Fig. 18, but they proposed an age of ~18 ka for this reconstruction, apparently based on the radiocarbon age of ~18.5 ka from the Troll site (Fig. 2). We thus consider that the geometry of the embayment shown in our Fig. 1 is in accordance with current interpretations of the glacial morphology. The main difference is that deglaciation of the eastern part of the North Sea according to our proposed chronology, which relies on the ^{10}Be ages from Utsira and Karmøy, took place earlier than proposed before. We also note that our alternative scenario, i.e. that an ice free corridor opened up across the entire North Sea in connection with the initial deglaciation, has been discussed by Clark et al. (2012).

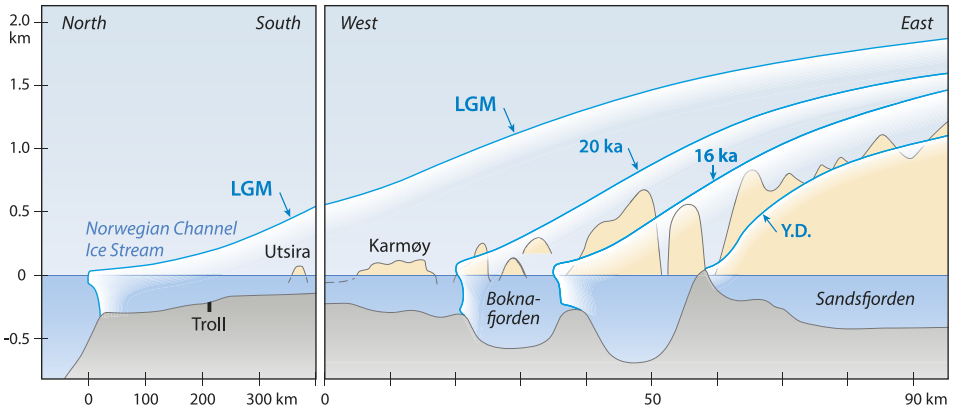

Fig. 8. Reconstructed ice-surface profiles. The inferred ice sheet profiles are drawn along the arrow shown in Fig. 2. Note the different distance scales between the N–S profile along the Norwegian Channel and the W–E profile up the fjords. The profile along the NCIS is modified from Sejrup et al. (2003); the profile of the Younger Dryas (YD) is from lateral moraines, whereas those in between are based on the YD profile.

5.3. Deglaciation after 20 ka

Our ^{10}Be ages from Tananger and Våg indicate that these areas were deglaciated ~16 ka, i.e. 4000 years after Utsira and the southern part of Karmøy became ice free, although the dated sites on the mainland are located only a short distance inland from the islands (Fig. 3). The ^{10}Be ages from Tananger are consistent with radiocarbon ages from lacustrine sediments farther south on Jæren (Fig. 2) that gave ages in the range 17–16 ka for deglaciation (Knudsen, 2006). Slightly younger ages have been obtained from lake basins near the eastern head of the narrow embayment Yrkjefjorden (Fig. 3) that was ice free ~15.5 ka (Anundsen, 1985; Braaten and Hermansen, 1985). A series of ^{10}Be ages from moraines located near the mouth of Lysefjorden indicate that large outlet glaciers of the ice sheet filled this fjord during the Older Dryas (~14 ka) and also during the later Younger Dryas advance (Briner et al., 2014). This means that almost all of Boknafjorden was ice-free when the ice front still was located close to the mouth of Hardangerfjorden farther to the north (Mangerud et al., 2013). This scenario is also consistent with the observed pattern of glacial striae suggesting that a wide calving bay developed in Boknafjorden at a time when the western margin of the Scandinavian Ice Sheet covered the coastal areas north of it (Rønnevik, 1971).

However, the exact position of the ice margin during the 4000-yr-long period between 20 and 16 ka is not known. In this regard we note that Karmsundet, the narrow and deep sound between Karmøy and the mainland (Fig. 3), contains glaciomarine sediments up to 250 m thick dating from the last deglaciation (Bøe et al., 2000). We suspect that this thick pile of sediments reflects a stillstand or a readvance of the ice front across the mouth of Boknafjorden. Olsen et al. (2013) reported six radiocarbon ages from shell fragments in till on northern Karmøy that yielded ages that ranged from 15.3 to 37.6 cal ka. Because of the large scatter of ages it is difficult to judge the reliability of individual ages and thus the real age of the till. However, if we discard the youngest age, they suggest that northern Karmøy was overridden by an ice sheet advance soon after 19–20 ka. The possibility that southern Karmøy has remained permanently ice free since about 20 ka whereas the northern part of the island was overridden by a later ice sheet advance is not contradicted by available observations, but new investigations are necessary to test out this assumption and to establish where the ice front was located during this time period.

5.4. Possible causal factors for the early deglaciation

The possible triggering mechanisms for the breakup of the NCIS may be changes in internal dynamics of the ice sheet, relative sea-level rise, increased surface melting and increased melting and/or calving of the marine margin. Glacial striae on summits in western Norway, especially close to the coast, show that ice flow during the maximum ice sheet extent was directed due west or slightly northwest, which are directions independent of fjords and other local topography. This implies that ice flow was determined by the surface gradient of the ice sheet independent of the underlying topography, including deep fjords and valleys. This pattern suggests that a thick ice sheet must have covered all coastal mountains on the mainland. The ice dome over southern Norway seems to have reached a level above 1700 m a.s.l. during the Younger Dryas period (Mangerud et al., 2013) and considering the distance between the positions of the ice margin during the Younger Dryas and the LGM we assume that it was several hundred metres higher than this during the LGM. It should be noted that ^{10}Be ages of erratics in the southern Norwegian mountains suggest that all, or at least almost all, mountain summits were ice covered at this time (Goehring et al., 2008).

There is evidence to suggest that the NCIS operated only periodically during the major glaciations (Sejrup et al., 2003). Both during the Kattegat glacier advance (~29–27 ka) and the Main stage (~23–21 ka) erratics from Norway were transported southward across the Norwegian Channel and onto Denmark (Houmark-Nielsen and Kjær, 2003; Larsen et al., 2009). We find it likely that the Scandinavian Ice Sheet at this time also was flowing westward across the Norwegian Channel and onto the shallow North Sea where it was merging with the British Ice Sheet (Mangerud, 2004) (Fig. 1). Later during the LGM, when the fast-flowing NCIS came into operation, the export of glacier ice across the Norwegian Channel must have been impeded. The fast flowing ice stream probably lowered the ice surface along the Norwegian Channel (Fig. 8) and thereby caused a drawdown of the entire ice sheet (Mangerud, 2004). We note that an early thinning of the ice sheet is supported by the low marine limit at Utsira suggesting that the ice load in this area was modest. Considering that the highest relative sea level on Utsira appears to have been less than 14–15 m a.s.l. implies that the glacioisostatic uplift has been less than 100 m since this island became ice free at ~20 ka.

A high flux of debris flow deposits on the North Sea Fan between 20 and 19 ka, which actually may have occurred a thousand years

earlier if our chronology is correct, indicates that the NCIS was active only during a brief period shortly before it started to breakup (Nygard et al., 2007). It remains uncertain which process initiated the ice streaming. It has been proposed that the rapid flow started at the mouth of the Norwegian Channel and then propagated upflow to form the NCIS (Mangerud, 2004). As mentioned above, the onset of the NCIS, running parallel with the coast of western Norway would cut off much of the ice supply to the North Sea, which is consistent with pre-20 ka ages for the North Sea becoming ice-free (Fig. 1). Furthermore, a consequence of the drawdown of the ice surface would be that a larger area came below the equilibrium line and thus leading to a more negative mass balance of the ice sheet. One may also add that the postulated thinning facilitated a more rapid calving of the ice stream and thereby also contributed to a rapid breakup of the remaining ice mass on the shelf west of the Norwegian Channel.

It has generally been suggested that rising sea level could be a triggering mechanism for destabilizing marine ice margins. This may have been the case during periods when the sea-level rise was exceptionally fast. However, the sea level rate of change in the far-field areas at low latitudes appears to have been rather slow (<1–2 mm/yr) during the period between 22 and 19 ka (Yokoyama et al., 2000; Peltier and Fairbanks, 2006; Hanebuth et al., 2009). In fact, relative sea level along the margin of the ice sheets may actually have been falling due to glacioisostatic uplift and loss of gravitational attraction as ice sheets thinned (Milne and Mitrovica, 2008). At any rate, it is well demonstrated that relative sea level along the west coast of Norway was falling during later stages of the deglaciation when the mean global eustatic sea level was rising much faster than during the initial deglaciation (Mangerud et al., 2013).

A similarly early retreat of the Scandinavian Ice Sheet has been recorded in northern Norway, where the island Andøya appears to have become ice free around 22 ka (Vorren et al., 2013). The British–Irish Ice Sheet was also thinning at this time even though the mass loss appears to have been rather slow until about 19 ka, when a much more rapid disintegration of the remaining ice sheet started (Clark et al., 2012). The fact that several glaciers and ice sheets in the Northern Hemisphere began to shrink at approximately at the same time (20–19 ka) suggests that the primary forcing mechanism was increasing high-northern-latitude insolation (Alley et al., 2005; Clark et al., 2009) rather than rising atmospheric CO_2 (Shakun et al., 2013). The ice core records from Greenland suggest that the climate there remained cold throughout the LGM, but a general warming seems to have been underway as early as about 21 ka when a geographic shift in the moisture source appears to have taken place (NGRIP Members, 2004; Masson-Delmotte, 2005).

Evidence in the Norwegian Sea suggests that relatively short-lived variations of sea ice cover and surface temperature took place even during the LGM, perhaps with episodic advection of warmer Atlantic surface water (de Vernal et al., 2005, 2006). However, the various proxy data from the Norwegian Sea are to some degree contradicting each other about LGM conditions. For example, planktonic foraminifer assemblages and $\delta^{18}O$ of *Neogloboquadrina pachyderma* shells suggest that rather low sea surface temperatures of about 4 °C or less prevailed during the summer seasons, whereas other proxy data (dinoflagellate cysts, coccoliths, alkenones and Mg/Ca ratios) point to much higher surface temperatures in the range of 10–14 °C (de Vernal et al., 2005, 2006; Meland et al., 2005). In sediment cores from the sea floor around the Faroe Islands, the first oceanic manifestation of the deglaciation seems to have occurred at 18–19 ka and is reflected as a temporary cooling of the surface water and increased sea ice cover (Rasmussen et al., 2002). However, biostratigraphic data from a well-dated sediment core from the continental slope to the west of Norway suggest that relatively warmer conditions may have prevailed in this part of the Norwegian Sea between 19.7 and 18.6 ka (Lekens et al., 2005). If real, this pulse of warmer water along the ice margin would have increased the melting and calving.

Stabilization of the ice front near the outer coast between 20 and 16 ka suggests that the south-western Scandinavian Ice Sheet was in balance during this interval. Pollen stratigraphic data, even though poorly constrained by radiocarbon ages, suggest that a cold and dry climate prevailed throughout this period (Paus, 1989b; 1990). Ice sheet retreat after 16 ka predates the Bølling interstadial that according to the Greenland ice core stratigraphy started at 14.7 ka (Andersen et al., 2006).

6. Conclusions

- The main conclusion is that ^{10}Be ages reveal that the margin of the Norwegian Channel Ice Stream (NCIS) had retreated 400 km from its LGM position by ~20 ka, i.e. about 2000 years earlier than previously thought.
- Together with ages from marine cores from the Fladen area about 250 km farther southwest (Fig. 1), our dating results suggest that the sea floor across most of the northern North Sea has was ice free as early as ~20 ka.
- The coastal areas slightly east of the islands Utsira and Karmøy became ice free at ~16 ka, indicating that there was little net ice sheet retreat between ~20 and ~16 ka.
- The Scandinavian Ice Sheet probably reached its maximum thickness before the NCIS came into operation and caused a lowering of the ice surface and also cut off ice flow to the North Sea.

Acknowledgements

The investigations form part of the research project Eurasian Ice Sheet and Climate Interaction (EISCLIM) financially supported by the Research Council of Norway (project no. 229788/E10). Lundin Norway AS provided funding of the ^{10}Be analysis and the Leiv Eiriksson Mobility Programme of the Research Council of Norway provided travel support for the investigators from USA. Stefan Truex at the University of Buffalo Cosmogenic Nuclide Laboratory assisted with sample preparation. Susan Zimmerman and Robert Finkel provided exceptional ^{10}Be AMS measurements at the Lawrence Livermore National Laboratory. Eva Bjørseth at the University of Bergen prepared the illustrations. Ed King and an anonymous reviewer provided useful comments and suggestions that helped to improve the quality of the manuscript. We offer our sincere thanks to all who have contributed to this study.

References

Aarseth, I., Mangerud, J., 1974. Younger Dryas end moraines between Hardangerfjorden and Sognefjorden, western Norway. Boreas 3, 3–22.
Alley, R.B., Clark, P.U., Huybrechts, P., Joughin, I., 2005. Ice-sheet and sea-level changes. Science 310, 456–460.
Andersen, B.G., Mangerud, J., Sorensen, R., Reite, A., Sveian, H., Thoresen, M., Bergstrom, B., 1995. Younger-Dryas ice-marginal deposits in Norway. Quat. Int. 28, 147–169.
Andersen, K.K., Svensson, A., Johnsen, S.J., Rasmussen, S.O., Bigler, M., Röthlisberger, R., Ruth, U., Siggaard-Andersen, M.-L., Peder Steffensen, J., Dahl-Jensen, D., 2006. The Greenland Ice Core chronology 2005, 15–42 ka. Part 1: constructing the time scale. Quat. Sci. Rev. 25, 3246–3257.
Anundsen, K., 1985. Changes in shore-level and ice-front position in Late Weichsel and Holocene, Southern Norway. Nor. Geogr. Tidsskr. 39, 205–225.
Anundsen, K., 1989. Late Weichselian relative sealevel in southwestern Norway: observed strandline tilts and neotectonic activity. Geol. Förenin. Stockh. Förhand. 111, 288–292.
Applegate, P.J., Urban, N.M., Keller, K., Lowell, T.V., Laabs, B.J.C., Kelly, M.A., Alley, R.B., 2012. Improved moraine age interpretations through explicit

matching of geomorphic process models to cosmogenic nuclide measurements from single landforms. Quat. Res. 77, 293–304.
Austad, R., Eriksen, C., 1987. Strandforskyvning på Nord-Karmøy basert på pollen og diatom e-analyse (Cand scient. thesis). University of Bergen, Norway.
Balco, G., Stone, J.O., Lifton, N.A., Dunai, T.J., 2008. A complete and easily accessible means of calculating surface exposure ages or erosion rates from ^{10}Be and ^{26}Al measurements. Quat. Geochronol. 33, 174–195.
Balco, G., Briner, J., Finkel, R.C., Rayburn, J.A., Ridge, J.C., Schaefer, J.M., 2009. Regional beryllium-10 production rate calibration for late-glacial northeastern North America. Quat. Geochronol. 4, 93–107.
Bennett, M.R., 2003. Ice streams as the arteries of an ice sheet: their mechanics, stability and significance. Earth Sci. Rev. 61, 309–339.
Bøe, R., Hovland, M., Instanes, A., Rise, L., Vasshus, S., 2000. Submarine slide scars and mass movements in Karmsundet and Skudenesfjorden, southwestern Norway: morphology and evolution. Mar. Geol. 167, 147–165.
Braathen, A.M., Hermansen, D., 1985. En Litho- og biostratigrafisk undersøkelse av marine og limniske sedimenter i Yrkje, Nord-Rogaland (Cand. scient. thesis). University of Bergen, Norway.
Bradwell, T., Stoker, M.S., Golledge, N.R., Wilson, C.K., Merritt, J.W., Long, D., Everest, J.D., Hestvik, O.B., Stevenson, A.G., Hubbard, A.L., Finlayson, A.G., Mathers, H.E., 2008. The northern sector of the last British Ice Sheet: maximum extent and demise. Earth Sci. Rev. 88, 207–226.
Briner, J.P., Svendsen, J.I., Mangerud, J., Lohne, Ø.S., Young, N.E., 2014. A ^{10}Be chronology of south-western Scandinavian Ice Sheet history during the Lateglacial period. J. Quat. Sci. 29, 370–380.
Clark, P.U., Dyke, A.S., Shakun, J.D., Carlson, A.E., Clark, J., Wohlfarth, B., Mitrovica, J.X., Hostetler, S.W., McCabe, A.M., 2009. The last glacial maximum. Science 325, 710–714.
Clark, C.D., Hughes, A.L.C., Greenwood, S.L., Jordan, C., Sejrup, H.P., 2012. Pattern and timing of retreat of the last British-Irish Ice Sheet. Quat. Sci. Rev. 44, 112–146.
de Vernal, A., Eynaud, F., Henry, M., Hillaire-Marcel, C., Londeix, L., Mangin, S., Matthiessen, J., Marret, F., Radi, T., Rochon, A., Solignac, S., Turon, J.L., 2005. Reconstruction of sea-surface conditions at middle to high latitudes of the Northern Hemisphere during the Last Glacial Maximum (LGM) based on dinoflagellate cyst assemblages. Quat. Sci. Rev. 24, 897–924.
de Vernal, A., Rosell-Melé, A., Kucera, M., Hillaire-Marcel, C., Eynaud, F., Weinelt, M., Dokken, T., Kageyama, M., 2006. Comparing proxies for the reconstruction of LGM sea-surface conditions in the northern North Atlantic. Quat. Sci. Rev. 25, 2820–2834.
Goehring, B.M., Brook, E.J., Linge, H., Raisbeck, G.M., Yiou, F., 2008. Beryllium-10 exposure ages of erratic boulders in southern Norway and implications for the history of the Fennoscandian Ice Sheet. Quat. Sci. Rev. 27, 320–336.
Goehring, B.M., Lohne, Ø.S., Mangerud, J., Svendsen, J.I., Gyllencreutz, R., Schaefer, J., Finkel, R., 2012. Late glacial and Holocene ^{10}Be production rates for western Norway. J. Quat. Sci. 27, 89–96.
Gosse, J.C., Phillips, F.M., 2001. Terrestrial in situ cosmogenic nuclides: theory and application. Quat. Sci. Rev. 20, 1475–1560.
Graham, A.G.C., Lonergan, L., Stoker, M.S., 2010. Depositional environments and chronology of Late Weichselian glaciation and deglaciation in the central North Sea. Boreas 39, 471–491.
Hafsten, U., 1983. Shore-level changes in South Norway during the last 13,000 years, traced by biostratigraphic methods and radiometric datings. Nor. Geogr. Tidsskr. – Nor. J. Geogr. 37, 63–79.
Hanebuth, T.J.J., Stattegger, K., Bojanowski, A., 2009. Termination of the Last Glacial Maximum sealevel lowstand: the Sunda-shelf data revisited. Glob. Planet. Change 66, 76–84.
Helle, S.K., 2006. Early Post-deglaciation Shorelines and Sea-level Changes along Hardangerfjorden and Adjacent Fjord Areas, W Norway (Dr. scient thesis). University of Bergen.
Holtedahl, H., 1975. The geology of Hardangerfjord, West Norway. Nor. Geol. Unders. 323, 1–87.
Houmark-Nielsen, M., Kjær, K., 2003. Southwest Scandinavia, 40–15 kyr BP: paleogeography and environmental change. J. Quat. Sci. 18 (8), 769–786.
Karlsen, L.C., 2009. Lateglacial vegetation and environment at the mouth of Hardangerfjorden, western Norway. Boreas 38, 315–334.
King, E.L., Haflidason, H., Sejrup, H.P., Lovlie, R., 1998. Glacigenic debris flows on the North Sea Trough Mouth Fan during ice stream maxima. Mar. Geol. 152, 217–246.
Knudsen, C.G., 2006. Glacier Dynamics and Lateglacial Environmental Changes – Evidences from SW Norway and Iceland (Dr. scient. thesis). University of Bergen.
Lal, D., 1991. Cosmic ray labeling of erosion surfaces: in situ nuclide production rates and erosion models. Earth Planet. Sci. Lett. 104, 424–439.
Larsen, N.K., Knudsen, K.L., Krohn, C.F., Kronborg, C., Murray, A.S., Nielsen, O.B., 2009. Late Quaternary ice sheet, lake and sea history of southwest Scandinavia – a synthesis. Boreas 38, 732–761.
Lekens, W.A.H., Sejrup, H.P., Haflidason, H., Petersen, G.Ø., Hjelstuen, B., Knorr, G., 2005. Laminated sediments preceding Heinrich event 1 in the Northern North Sea and Southern Norwegian Sea: origin, processes and regional linkage. Mar. Geol. 216, 27–50.
Lohne, Ø.S., Mangerud, J., Svendsen, J.I., 2011. Timing of the Younger Dryas glacial maximum in western Norway. J. Quat. Sci. 27, 81–88.
Mangerud, J., 2004. Ice sheet limits on Norway and the Norwegian continental shelf. In: Ehlers, J., Gibbard, P. (Eds.), Quaternary Glaciations – Extent and Chronology, vol. 1. Elsevier, Amsterdam, Europe, pp. 271–294.
Mangerud, J., Goehring, B.M., Lohne, Ø.S., Svendsen, J.I., Gyllencreutz, R., 2013. Collapse of marine-based outlet glaciers from the Scandinavian Ice Sheet. Quat. Sci. Rev. 67, 8–16.
Masson-Delmotte, V., Jouzel, J., Landias, A., Stievenard, M., Johnsen, S.J., White, J.W.C., Werner, M., Sveinbjornsdottir, A., Fuhrer, K., 2005. GRIP deuterium excess reveals rapid and orbital-scale changes in Greenland moisture origin. Science 309, 118–121.
Meland, M.Y., Jansen, E., Elderfield, H., 2005. Constraints on SST estimates for the northern North Atlantic/Nordic Seas during the LGM. Quat. Sci. Rev. 24, 835–852.
Milne, G.A., Mitrovica, J.X., 2008. Searching for eustasy in deglacial sea-level histories. Quat. Sci. Rev. 27, 2292–2302.
NGRIP Project Members, 2004. High-resolution record of Northern Hemisphere climate extending into the last interglacial period. Nature 431, 147–151.
Nishiizumi, K., Imamura, M., Caffee, M.W., Southon, J.R., Finkel, R.C., McAninch, J., 2007. Absolute calibration of ^{10}Be AMS standards. Nucl. Instrum. Methods Phys. Res. Sect. B – Beam Interact. Mater. Atoms 258, 403–413.
Nygard, A., Sejrup, H.P., Haflidason, H., Lekens, W.A.H., Clark, C.D., Bigg, G.R., 2007. Extreme sediment and ice discharge from marine-based ice streams: new evidence from the North Sea. Geology 35, 395–398.
Olsen, L., Sveian, H., Ottesen, D., Rise, L., 2013. Quaternary glacial, interglacial and interstadial deposits of Norway and adjacent onshore and offshore areas. In: Olsen, L., Fredin, L., Olesen, O. (Eds.), Quaternary Geology of Norway, Geological Survey of Norway Special Publication, vol. 13, p. 173.
Ottesen, D., Dowdeswell, J.A., Rise, L., 2005. Submarine landforms and the reconstruction of fast-flowing ice streams within a large Quaternary ice sheet: the 2500-km-long Norwegian-Svalbard margin (57°–80°N). Geol. Soc. Am. Bull. 117, 1033–1050.
Paus, Aa, 1988. Late Weichselian vegetation, climate and floral migration at Sandviksvatnet, North Rogaland, southwestern Norway. Boreas 17, 113–139.
Paus, Aa, 1989a. Late Weichselian vegetation, climate, and floral migration at Liastemmen, North Rogaland, south-western Norway. J. Quat. Sci. 4, 223–242.
Paus, Aa, 1989b. Late Weichselian vegetation, climate, and floral migration at Eigebakken, South Rogaland, southwestern Norway. Rev. Paleobot. Palynol. 61, 177–203.
Paus, Aa, 1990. Late Weichselian and early Holocene vegetation, climate and floral migration at Utsira, North Rogaland, southwestern Norway. Nor. Geol. Tidsskr. 70, 135–152.
Peltier, W.R., Fairbanks, R.G., 2006. Global glacial ice volume and Last Glacial Maximum duration from an extended Barbados sea level record. Quat. Sci. Rev. 25, 3322–3337.
Pritchard, H.D., Arthern, R.J., Vaughan, D.G., Edwards, L.A., 2009. Extensive dynamic thinning on the margins of the Greenland and Antarctic ice sheets. Nature 461, 971–975.
Ragnhildstveit, E., Naterstad, J., Jorde, K., Egeland, B., 1998. Geologisk kart over Norge, begrunnskart Haugesund, 1:250000. Norges Geologiske Undersøkelse.
Rasmussen, T.L., Bäckström, D., Heinemeier, J., Klitgaard-Kristensen, D., Knutz, P.C., Kuijpers, A., Lassen, S., Thomsen, E., Troelstra, S.R., Van Weering, T., 2002. The Faroe-Shetland Gateway: Late Quaternary water mass exchange between the Nordic seas and the northeastern Atlantic. Mar. Geol. 188, 165–192.
Ringen, E., 1964. Om drumliner og Skagerakmorene på Karmøy. Nor. Geogr. Tidsskr. 19, 205–228.
Rise, L., Bøe, R., Ottesen, D., Longva, O., Olsen, H.A., 2008. Postglacial depositional environments and sedimentation rates in the Norwegian Channel off southern Norway. Mar. Geol. 251, 124–138.
Rønnevik, H.K., 1971. Kvartærgeologi på ytre del av Haugesunsdhalvøya (Cand. real thesis). University of Bergen.
Rood, D.H., Hall, S., Guilderson, T.P., Finkel, R.C., Brown, T.A., 2010. Nucl. Inst. Methods Phys. Res. B 268, 730–732.
Sejrup, H.P., Haflidason, H., Aarseth, I., King, E., Forsberg, C.F., Long, D., Rokoengen, K., 1994. Late Weichselian glaciation history of the Northern North-Sea. Boreas 23, 1–13.
Sejrup, H.P., Landvik, J.Y., Larsen, E., Janocko, J., Eiriksson, J., King, E., 1998. The Jæren area, a border zone of the Norwegian channel ice stream. Quat. Sci. Rev. 17, 801–812.
Sejrup, H.P., Larsen, E., Haflidason, H., Berstad, I.M., Hjelstuen, B.O., Jonsdottir, H.E., King, E.L., Landvik, J., Longva, O., Nygård, A., Ottesen, D., Raunholm, S., Rise, L., Stalsberg, K., 2003. Configuration, history and impact of the Norwegian Channel Ice Stream. Boreas 32, 18–36.
Sejrup, H.P., Nygard, A., Hall, A.M., Haflidason, H., 2009. Middle and Late Weichselian (Devensian) glaciation history of south-western Norway, North Sea and eastern UK. Quat. Sci. Rev. 28, 370–380.
Sejrup, H.P., Hjelstuen, B., Nygård, A., Haflidason, H., Mardal, I., 2014. Late Devensian ice-marginal features in the central North Sea – processes and chronology. Boreas. http://dx.doi.org/10.1111/bor.12090 (in press).
Shakun, J.D., Clark, P.U., He, F., Marcott, S.A., Mix, A.C., Liu, Z., Otto-Bliesner, B., Schmittner, A., Bard, E., 2013. Global warming preceded by increasing carbon dioxide concentrations during the last deglaciation. Nature 484, 49–54.
Staiger, J., Gosse, J., Toracinta, R., Oglesby, B., Fastook, J., Johnson, J.V., 2007. Atmospheric scaling of cosmogenic nuclide production: climate effect. J. Geophys. Res. 112, B02205.
Stokes, C.R., Clark, C.D., 2001. Palaeo-ice streams. Quat. Sci. Rev. 20, 1437–1457.

Stone, J.O., 2000. Air pressure and cosmogenic isotope production. J. Geophys. Res. 105, 23753–23759.
Svendsen, J.I., Alexanderson, H., Astakhov, V.I., Demidov, I., Dowdeswell, J.A., Funder, S., Gataullin, V., Henriksen, M., Hjort, C., Houmark-Nielsen, M., Hubberten, H.W., Ingolfsson, O., Jakobsson, M., Kjær, K.H., Larsen, E., Lokrantz, H., Lunkka, J.P., Lysså, A., Mangerud, J., Matiouchkov, A., Murray, A., Möller, P., Niessen, F., Nikolskaya, O., Polyak, L., Saarnisto, M., Siegert, C., Siegert, M.J., Spielhagen, R.F., Stein, R., 2004. Late Quaternary ice sheet history of northern Eurasia. Quat. Sci. Rev. 23, 1229–1271.
Thomsen, H., 1981. Late Weichselian shore-level displacement on Nord-Jæren, south-west Norway. Geol. Förenin. Stockh. Förhand. 103, 447–468.
Undås, I., 1948. Trekk fra Utsiras natur og den siste Skageraksbre. Stavangers Museums Årbok, pp. 59–71.
Vorren, T.O., Vorren, K.-D., Aasheim, O., Dahlgren, K.I.T., Forwick, M., Hassel, K., 2013. Palaeoenvironment in northern Norway between 22.2 and 14.5 cal. ka BP. Boreas 42, 876–895.
Yokoyama, Y., Lambeck, K., De Deckker, P., Johnston, P., Fifield, L.K., 2000. Timing of the Last Glacial Maximum from observed sea-level minima. Nature 406, 713–716.
Young, N.E., Schaefer, J.M., Briner, J.P., Goehring, B.M., 2013. A ^{10}Be production-rate calibration for the Arctic. J. Quat. Sci. 28, 515–526.